J. Condensed Matter Nucl. Sci. 19 (2016) 202–209

Research Article

Basis for Femto-molecules and -Ions Created from Femto-atoms

Andrew Meulenberg*
Science for Humanity Trust Inc., USA

Jean-Luc Paillet
Aix-Marseille University, France

Abstract

Starting with the assumption of validity of the Dirac equations (relativistic quantum mechanics), which are fundamental to much of atomic physics today, we also assume that the anomalous solutions to these equations are valid. If they are valid, then short-lived femto-atoms with electron orbitals in the low femto-meter range should exist. If femto-atoms exist, then the existence of femto-molecules could be expected. This paper addresses the possibility and nature of the femto-molecules and the nature of the forces creating them. The approach is that of Feynman's molecular-hydrogen ion derivation using the Yukawa potential. The result is a molecular ion with femto-meter order spacing between the nuclei and an attractive potential identical with a medium-range Yukawa potential for an exchange particle with the mass of an electron. There are significant implications for both cold fusion and for nuclear physics and chemistry.
 ISSN 2227-3123

Keywords: Deep-Dirac levels, Femto-hydrides, Halo nuclei, Isotopic anomalies, Medium-range nuclear binding

1. Introduction

Given the existence of femto-hydrogen atoms with electrons in Deep-Dirac Levels (DDLs) having binding energies at 509 keV [1], what support can be given for the existence of molecules composed of such atoms? Starting with Feynman's quantum mechanical, but non-relativistic, derivation of the molecular-hydrogen ion [2], we will extend it to the femto-meter and relativistic region – to the femto-molecular level.

2. Feynman's Derivation of H_2^+ Molecular-ions based on Electron-exchange Potentials

Feynman assumes a paired two-state system consisting of two protons and an electron. A primary potential E_0 is the electron-screened repulsive Coulomb potential between the protons. Secondary potentials, $\pm A$,exist because the electron can be exchanged between the two protons in two ways (with $A < 0$). Two resulting time-independent states

*E-mail: mules333@gmail.com

 ISSN 2227-3123

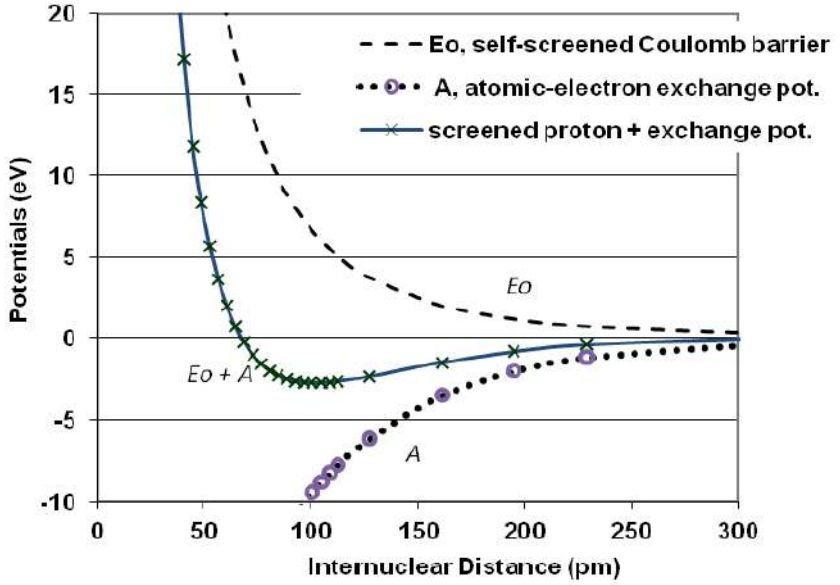

Figure 1. Potentials, as a function of internuclear separation, between two protons with a bound electron.

of the system (EI and EII) are composed of the primary potential, E_0, plus the secondary potential (A or $-A$). Since in one case, the summed potential is always repulsive, no bound state can exist. In the other case, the summed potential has a region of negative energy – the bound state. Figure 1 provides sample values of these potentials based on the H_2^+ ion.

Feynman does not go into the details of the screened potential, so neither shall we [3]. However, the critical issue for us is the nature of the 'exchange' potential, A. The unlabeled precursor to his equation (Eq. (10.10)) for this term is the amplitude for a free particle to get from one place to another a distance R away:

$$A \sim (1/R)\exp(ipR/\hbar), \tag{1}$$

where p is the momentum of the electron [4] and R is the distance between the protons. (Notice that p/h is just 2π divided by the deBroglie wavelength, λ_{dB}.) For a non-relativistic atomic electron with mass, m, and kinetic energy, KE, its momentum $p = (2m\,\mathrm{KE})^{1/2}$. However, when encountering a barrier and tunneling into or through it, the wave equation predicts an increase in deBroglie wavelength of the particle as its momentum goes toward zero at the barrier. At the barrier, the wavelength goes to infinity and the wave function turns into a reflection from, and an exponentially decaying function (an evanescent wave) inside, the barrier.

For a particle trapped in a well, where its potential (relative to outside the well) is less than zero, $V < 0$, the kinetic energy, $\mathrm{KE} = \mathrm{TE} - V$, is a positive value equal to the difference between the total energy, TE, and the potential energy ($V < \mathrm{TE} < 0$). However, if the particle tries to penetrate the wall of the well, where $V = 0$, then $\mathrm{KE} = \mathrm{TE} < 0$. As a result and since $\mathrm{KE} < 0$, the momentum p is imaginary:

$$p = (2m\mathrm{KE})^{1/2} = (2m(\mathrm{TE} - V))^{1/2} \quad \text{and} \quad \mathbf{p}=\mathbf{i}(2\mathbf{m}|\mathbf{TE}|)^{1/2} \text{for } V = 0 \text{ and } \mathrm{TE} < 0. \tag{2}$$

The non-relativistic virial theorem for particles bound in a Coulomb $(1/r)$ potential states that KE $=$ PE$/2$ for stable orbits. Since the difference between total energy and potential energy is the binding energy BE of the trapped particle, a positive energy equal to the absolute value of the binding energy, $|\mathrm{BE}| = |\mathrm{TE} - V|$, is necessary to lift the particle out of the well. For a bound particle, the potential outside of the well (amplitude for penetrating into the barrier), no longer with the imaginary exponent, is

$$A \sim (1/R)\exp((-(2m|\mathrm{BE}|)^{1/2}/\hbar)R). \tag{3}$$

In his 'Lectures' [2], Feynman used W_H for the binding energy of the hydrogen electron (W_H is the work required to take an electron from the H-atom ground state to infinity) but, outside of the well (where $V = 0$), he set BE equal to the negative of the kinetic energy in the well (KE $= -$BE). Thus, he was able to make p imaginary and arrived at the same operative expression for the exchange potential, Eq. (3).

3. H_2^+ Femto-molecular-ion Electron-exchange Potentials

The DDL-electron exchange effect produces a much shorter-range attractive potential than does the atomic-electron effect. In Fig. 2, the log-log version of Fig. 1, the primary potential E_0 is again the electron-screened repulsive Coulomb potential between the protons and, here, it only represents the effect of loosely bound (5.8 eV) molecular-orbit electrons. The absolute values of various attractive exchange potentials (A, A_2, and $A_2' < 0$) are displayed so that their magnitudes can be compared directly against the repulsive potentials.

The attractive secondary potentials for molecular- and DDL-electron orbits (A, A_2, and A_2') indicate the differences between the bound-electrons of different average kinetic energies (5.8 eV, 100 keV, and 1.5 MeV, respectively). The reason that they, unlike the E_0 curve, 'flatten out' (saturate) below the picometer- and lower-fermi-ranges respectively is related to the facts that E_0 is the electron-screened proton–proton Coulomb repulsion and that the A's are for the proton–electron interaction. The 'size' of the electron orbital distribution exceeds the spatial separation

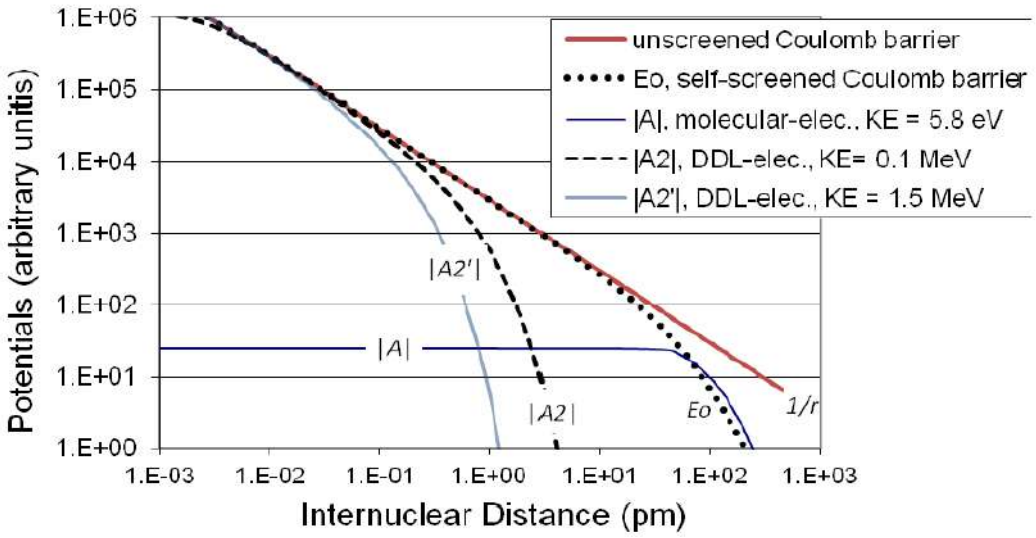

Figure 2. Representative potentials (some from Fig. 1 but now on a log-log plot) as a function of internuclear separation, between two protons with a bound electron.

between the protons within this range and therefore the screening is reduced as the protons come together and the electron spends less and less time between the protons. The DDL orbitals in the low femto-meter range means that the screening-saturation effect does not really begin until the protons get within the sub-picometer range of one another.

This exchange-particle range is based on the particle's momentum (as in the deBroglie wavelength and Eq. (1)). In the Yukawa nuclear potential, the relativistic momentum is related to the mass energy, $E^2 = (pc)^2 + (mc^2)^2$ and, with the assumption of total energy near zero, $E =\sim 0$, leading to $p =\sim imc$, the resulting potential has a range dependence on the particle's Compton wavelength, λ_C (Feynman's Eq. (10.14)).

$$A\sim (1/R)\exp(-mc/\hbar)R= (1/R)\exp(-2\pi R/\lambda_C) \tag{4}$$

This equation is the basis of both the short-range pion-exchange force and the long-range photon-exchange model. However, in Feynman's electron-exchange model of the molecular binding potential, the non-relativistic equation for momentum relates it to the square root of the kinetic energy, $p = (2m\,\mathrm{KE})^{1/2}$– and that to the binding energy (Eq. (3)).

The femto-molecule analysis is in-between the strongly relativistic and the non-relativistic regimes. The relativistic momentum is still strongly related to the electron mass energy, $E^2 = (pc)^2 + (mc^2)^2$, since E, at 2–4 keV (depending of whether the Dirac or Klein–Gordon anomalous solutions are used) [5] for the hydrogen atom, is much smaller than mc^2 (at 511 keV). The main differences between the atomic molecule and the femto-molecule are in the greatly increased screening provided by the deep electron orbits (reducing the range of E_0) and in the greatly enhanced exchange potential as seen with A_2 and A_2' in Fig. 2.

Our analyses, of both the molecular and the femto-molecular ion exchange energies, are representative rather than accurate. They assume that the screening field of the electron in the molecule is twice the Bohr radius, $a_0 =\sim 53$ pm; but, for the femto-molecule, it is reduced to the classical electron radius, $r_e =\sim 2.8$ fm. The fact that the classical electron radius is the fine structure constant times the Compton electron radius, $r_C = \lambda_{dB}/2\pi$, and r_C is the fine structure constant times the Bohr electron radius makes one wonder about some sort of divine power-series expansion in 'α' :

$$r_e = \alpha r_C = \alpha^2 a_0. \tag{5}$$

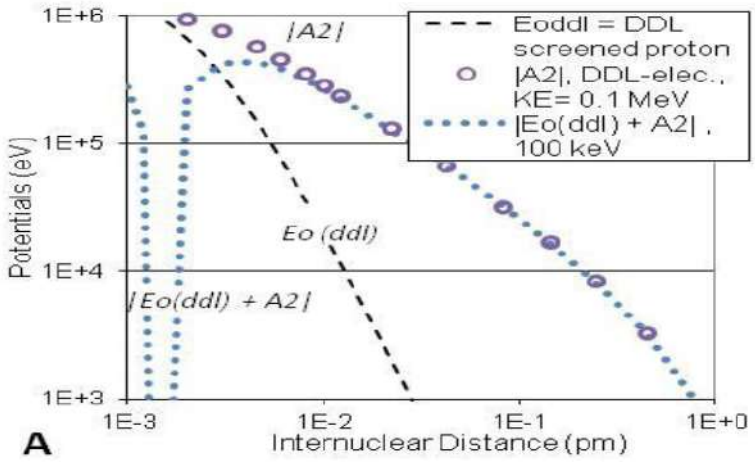

Figure 3. Log-log information for the screened Coulomb repulsion and the exchange potentials of femto-H_2^+ and their sums.

4. Summed Potentials of H_2^+ Femto-molecular-ions

Figure 3 is a log-log plot of the femto-molecular ranges (thus complementing the atomic-molecular range of Fig. 2). It has three curves that give an indication of the parameters to consider. The nuclear potential is ignored, since it would dominate if the spacing between protons reached that low. The unscreened Coulomb barrier (not shown) between the protons is the starting point. The presence of the electron provides a self-screening of that potential and this screened potential, E_0(ddl), is the one that is to be worked with. It is the femto-atom equivalent of E_0 in Feynman's model (and in Figs.1 and 2).

Comparison of the E_0 curves in Figs. 2 and 3 shows the effect of strong screening by a DDL electron vs that of an atomic electron. $|A_2|$ and the sum of the two potentials, $|E_0$ (ddl) + $A_2|$ in Fig 3, are displayed against the E_0 (ddl) curve to indicate explicitly their relative magnitude.

The absolute value of the exchange potential, $|A_2|$, is now much larger than the screened Coulomb potential E_0 (ddl) until the protons are within the multi-femto-meter range. The maximum attractive potential for the sum is at about 5 fm for the 100 keV electron kinetic energy in Fig. 3. In Fig 4, the electron KE is raised to $\sim$ 1.5 MeV (an expected value for a DDL electron) and the results are displayed on a semi-log plot for ease of interpretation. For this higher KE (A_2'), with a smaller average orbital radius that is in agreement with projected DDL electron orbits, the attractive summed potential is 'smeared' into the nucleus ($R < 1$ fm) and actual fusion of the protons to a deuteron could be unavoidable. However, there are things missing in this analysis, such as spin–spin coupling, which is very strong at this range and will alter the results; so what is shown is only indicative of expectation. Detailed calculations will have to await a more complete understanding of the proximity effects of the bound electron and proton.

A potentially important point in Fig. 4 is the solid curve (Yukawa exchange potential). While the nuclear potentials have been postulated to result from virtual pion-exchange (shorter range with much higher particle mass), an intermediate-range (100 fm) force has long-been proposed and sought (by one of the present authors, AM, and by Jacque Dufour [6]) to explain cold fusion. This mid-range force can be associated with the Yukawa potential for a

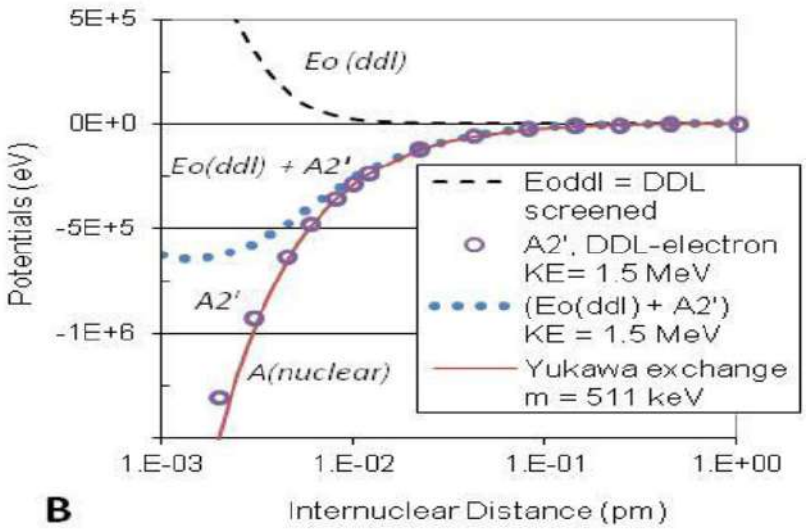

Figure 4. Semi-log information for the screened Coulomb repulsion and the exchange potentials of femto-H_2^+ and their sums. The Yukawa potential for a virtual-electron exchange is included.

real-electron-exchange mass of 511 keV/c^2. The A_2' curve is coincident with the Yukawa exchange potential until the low femto-meter range. This should not be a surprise. The contributions to both the A_2' and the Yukawa-exchange potentials are nearly identical except for the values of R. The $1/R$ values in Eq. (3) are based on the same distance between nuclei centers. However, the R value used in the exponent of the present model is a weighted average of the distances 'tunneled' between potential wells and this is slightly less than the distance between proton centers used in the Yukawa potential.

Such an intermediate-range attractive force could appear to be nuclear in nature, but much more extended; it would also provide a basis for the metastable halo nuclei [7]. The 'odd' nucleons (protons or neutrons) that are bound in the 5–8 fm range of a halo nucleus could be femto-hydrides.

5. Femto-molecular Hydrides and Experimental Data

The final issue, addressed here only with a quick comment, is that of the neutral femto-molecule. With two protons and two electrons, the attractive potential is much greater. As a first-order approximation to the problem, just double the DDL-electron attraction between the protons. The Coulomb repulsion between the electrons may be eliminated by the spin–spin attraction of the electron pair with anti-parallel spin vectors. Therefore, we may not have to be concerned about that otherwise major issue. If the electron-exchange potential is doubled by addition of the second deep-orbit electron, then this effect may dominate the other effects and a deeper or broader potential well results. Whether the well is metastable, or immediately leads to fusion, is still to be determined even from the simple case modeled.

What happens when a femto-H atom or femto-H_2 molecule forms within a lattice? This theoretical issue has now been partially addressed for transmutation [8,9]. Nevertheless, there have been some experimental transmutation results that, if valid, would appear to be self-contradictory. The first was from Defkalion where four of the natural isotopes of nickel (^{58}Ni, ^{60}Ni,^{61}Ni, and^{62}Ni), were used to test for excess heat [10]. All but ^{61}Ni, produced excess heat. Why did ^{61}Ni not do so (even when the experiment was repeated)? The second was from Rossi's system tests at Lugano [11], where the residual nickel isotope, after a month of producing excess heat, was ^{62}Ni. While both results would indicate nuclear fusion results, the apparent contradiction of the results could cast doubt on the whole process.

An attempt to understand the two results has provided suggestions that may or may not be valid. In the referenced Defkalion work, the ^{61}Ni is the only isotope tested that does not have a zero isotopic spin ground state. (It has $J = 3/2$, with negative parity.) What does this have to do with cold fusion? It is known that only low-angular-momentum states can result for/from low-incident-energy collisions. If these $H^{\#}$ states cannot interact with the high total angular momentum of the ^{61}Ni nucleus, then a femto-hydride is the preferred state (a chemical rather than a nuclear bond). The result is that the energy of formation of the femto-H atom or molecule (about 0.5 MeV per H) would be the only excess energy that could result from this formation of the femto-hydride. While there is still excess energy, it is much less than would result from the multi-MeV fusion or transmutation energies. Since cold fusion reactions in the nickel system increase with lattice temperature, it is possible that the ^{61}Ni test, with a much lower excess power ability, never achieved a critical level under the same test conditions that worked for the other isotopes. The test results are proprietary (and Defkalion is no longer in business), so that it is not possible to get more information, or actual samples, from those tests.

The Lugano test results showed a strong depletion of the natural ^{58}Ni, ^{60}Ni, ^{61}Ni, and ^{64}Ni isotopes. The ^{62}Ni was the main residual nuclide measured. There is no ready explanation for this observation that is consistent with the ^{61}Ni 'anomaly' and the reported results of the earlier experiment. However, there is a possible, and testable, explanation. The experimental results showing ^{62}Ni could in fact be a 'misreading' of the isotopic test results. While the equipment used was capable of very fine mass separation (e.g., resolution of adjacent isotopes), there is a real possibility that a slight shift in a strong peak could have been overlooked even if the high resolution mode were employed in test. The ^{62}Ni peak and the ^{61}Ni + $H^{\#}$ peak are probably within 10 MeV/c^2 of each other. The shift of the peak from ^{62}Ni to

^{61}Ni + H$^{\#}$ would not normally be expected and therefore would not be noticed. Had there been a residue of ^{62}Ni, the doublet would have been obvious if measurements were taken at the full resolution of the test equipment. Again, this is proprietary data and material samples, so neither may become available for further testing and analysis until 'profit' warrants it.

6. Conclusion

Using a text-book derivation for the diatomic-molecular ion, we have derived the bound-state solution for a pair of protons bound together by a deep-level electron. The present approach combines that of the molecular-binding problem using real charged particles, the electron, with that of the nuclear-binding problem using the Yukawa potential and virtual particles, the pion. The high binding energy of the deep-level electrons (~ 500 keV), is closer to that of the nuclear forces (multi-MeV) than that of the atomic forces (multi-eV); therefore, it is no surprise that the results for the femto-molecular ion appear to be that of a mid-range (i.e., ~ 100 fm) Yukawa nuclear-binding potential. In fact, the results are almost indistinguishable from those for nuclear binding based on virtual-electron exchange.

This similarity of forces leading to the femto-molecular ion with the nuclear forces and the conclusions from such similarity can lead to two quite different responses. First, the statement that "nuclear forces can be mediated only by gauge bosons" is too limiting. Second, "the proposed electron deep levels (EDLs) cannot exist;" therefore, "Feynman's molecular-ion derivation cannot be applied in this case." We cannot accept either part of the second statement. Just as the anomalous solutions of the relativistic Schrodinger and Dirac equations predict the existence of the EDLs [5,12,13], and thus femto-atoms [8], the analysis in this paper predicts the possibility of femto-molecules, femto-molecular ions, and medium-range nuclear binding by real electrons. Evidence of the existence of all these effects is strongly suggested by experimental evidence provided by results of the cold fusion work over the last 25+ years.

Acknowledgement

This work is supported in part by HiPi Consulting, New Market, MD, USA; by the Science for Humanity Trust, Bangalore, India; and by the Science for Humanity Trust, Inc, Tucker, GA, USA.

References

[1] J.A. Maly and J. Vavra, Electron transitions on deep Dirac levels I, *Fusion Technol.* **24** (1993) 307–381, http://people.web.psi.ch/pruchova/Vavra_d_dirac_l.pdf.
[2] R.P. Feynman, R.B, Leighton and M. Sands, *The Feynman Lectures on Physics*, Vol. 3, Chapter 10, Sections 1–3, Addison–Wesley, Reading, MA, USA, 1965.
[3] A. Deltuva, Coulomb force effects in low-energy α-deuteron scattering**,** *Phy. Rev.* C **74** (2006) 064001.
[4] R.P. Feynman, R.B, Leighton and M. Sands, *The Feynman Lectures on Physics*, Vol. 3, Chapter 3.1, Eq. (3-7), Addison–Wesley, Reading, MA, USA, 1965.
[5] Jean-Luc Paillet and Andrew Meulenberg, Arguments for the anomalous solutions of the Dirac equations, http://viXra.org/abs/1506.0177, *J. Condensed Matter Nucl. Sci.* **18** (2016) 50–75.
[6] J. Dufour, An introduction to the pico-chemistry working hypothesis, *J. Condensed Matter Nucl. Sci.* **10** (2013) 40–45.
[7] https://en.wikipedia.org/wiki/Halo_nucleus.
[8] A. Meulenberg, Femto-atoms and transmutation, *ICCF-17*, Daejeon, South Korea, 12–17 August, 2012, *J. Condensed Matter Nucl. Sci.* **13** (2014) 346—357.
[9] A. Meulenberg, Femto-helium and PdD transmutation, *ICCF-18*, *18th Int. Conf. on Cond. Matter Nucl. Sci.*, Columbia, Missouri, 25/07/2013, http://hdl.handle.net/10355/36500.
[10] J. Hadjichristos, M. Koulouris and A. Chatzichristos, Technical characteristics and performance of the Defkalion's hyperion pre-industrial product, *17th Int. Conf. on Condensed Matter Nucl. Sci.*, Daejeon, South Korea, 12–17 August, 2012.

[11] G. Levi et al., Observation of abundant heat production from a reactor device and of isotopic changes in the fuel, http://amsacta.unibo.it/4084/, ecat.com/wp-content/uploads/2014/10/ECAT-test-report-2014.pdf, 2014.
[12] J.L. Paillet and A. Meulenberg, The basis for electron deep orbits of the hydrogen atom, *ICCF-19*, *19th Int. Conf. on Cond. Matter Nuclear Science*, Padua, Italy, 15/05/2015, to appear in *J. Condensed Matter Nucl. Sci.* **19** (2016).
[13] A. Meulenberg and J.L. Paillet, Nature of the deep-Dirac levels, *ICCF-19, 19th Int. Conf. on Cond. Matter Nucl. Sci*., Padua, Italy, 15/05/2015, to appear in *J. Condensed Matter Nucl. Sci.* **19** (2016).